de Haas-van Alphen effect investigations of the electronic structure of pure and aluminum-doped MgB_2

A. Carrington [a] E.A. Yelland [a] J.D. Fletcher [a] J.R. Cooper [b]

[a] *H. H. Wills Physics Laboratory, University of Bristol, Bristol, BS8 1TL, England.*
[b] *Department of Physics,University of Cambridge, Madingley Road, Cambridge, CB3 0HE, England.*

Abstract

Understanding the superconducting properties of MgB_2 is based strongly on knowledge of its electronic structure. In this paper we review experimental measurements of the Fermi surface parameters of pure and Al-doped MgB_2 using the de Haas-van Alphen (dHvA) effect. In general, the measurements are in excellent agreement with the theoretical predictions of the electronic structure, including the strength of the electron-phonon coupling on each Fermi surface sheet. For the Al doped samples, we are able to measure how the band structure changes with doping and again these are in excellent agreement with calculations based on the virtual crystal approximation. We also review work on the dHvA effect in the superconducting state.

Key words: MgB_2, Fermi surface, Band structure, Quantum oscillations
PACS:

1. Introduction

The physical properties of MgB_2 are strongly linked to its unusual electronic structure. This has been extensively investigated theoretically and has led to a detailed microscopic understanding of the physics of this material. Experimentally, there are many probes which are sensitive to various aspects of the anisotropic electronic structure, although there are relatively few which can determine the most fundamental parameters accurately. For example, measurements of the resistivity can be used to estimate the average mean-free-paths ℓ along the two principal crystallographic directions (a and c), but cannot provide $\boldsymbol{k}$-resolved information.

Knowledge of these $\boldsymbol{k}$-dependent parameters and how they vary with doping is important for understanding the superconducting properties of MgB_2, such as T_c and the upper critical field H_{c2}. In particular, a knowledge of how a certain dopant changes the band filling and the scattering rates on the various Fermi surface sheets can help in optimizing the superconducting properties for applications. For example, in order to raise H_{c2} it is necessary to lower the mean-free-path, especially on the σ sheets of the Fermi surface, which have a large superconducting gap, without depressing T_c too much by mixing in states from other parts of the Fermi surface where the gap is smaller.

The de Haas-van Alphen (dHvA) effect, is a powerful method for determining the Fermi surface parameters of metals, providing information about the size and shape of the Fermi surface sheets, and the scattering rates and quasiparticle effective masses on these sheets [1]. The data are usually interpreted using Lifshitz-Kosevich (LK) theory [1]. The main experimental constraint comes from the fact that dHvA oscillations are only observable if the quasiparticles complete a significant fraction of a cyclotron orbit before being scattered. In practice, high magnetic fields and reasonably pure

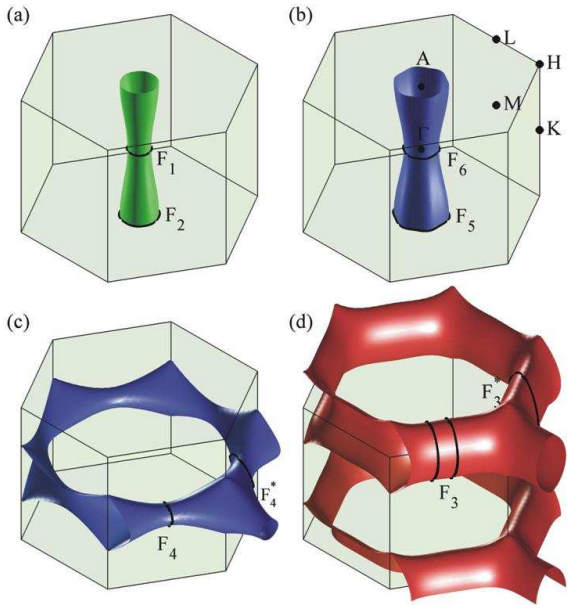

Fig. 1. (color) Calculated Fermi surface of MgB_2, with possible dHvA extremal orbits (for frequencies <10 kT) indicated. Panels (a)-(d) show the σ-light hole, σ-heavy hole, π-hole and π-electron bands respectively.

samples with long mean-free-paths are needed. This limits the study of doping effects on the electronic structure, since doping is usually achieved by partial atomic substitution which inevitably increases scattering and therefore decreases ℓ. The amplitude of the dHvA signal is reduced from its value in a perfectly clean sample by the Dingle factor [1], $R_D = \exp(-\frac{\pi}{\omega_c \tau}) = \exp(-\frac{\pi \hbar k_F}{eB\ell})$. The damping is increased with shorter ℓ and increased average Fermi wavevector (k_F) of the orbit (or equivalently as the product of the cyclotron frequency ω_c and the scattering time τ decreases). This can be offset, to some extent, by making measurements at very high magnetic fields B, although in practice, we are still limited to dopant levels of a few atomic percent where the increase in scattering is not too severe.

In this paper we will review studies of the dHvA effect in both pure and aluminum doped MgB_2, and information obtained about the electronic structure and superconducting properties.

2. Electronic structure

The interpretation of dHvA data is considerably aided by detailed comparison with band structure calculations. The first calculations of the band structure of MgB_2 were reported long before the discovery of superconductivity in MgB_2 (see Ref. [2]). Shortly after the discovery of superconductivity, Kortus *et al.* [3] reported detailed calculations of the Fermi surface which specifically address the issue of the origin of the superconductivity. Since then there have been a large number of other reports which have confirmed and added to this picture (see for example, Refs. [4,5,6,7,8]).

Generally, the electronic orbits which give rise to dHvA oscillations are located at the points where there is a local minimum or maximum in the Fermi surface cross-sectional area along the direction of the applied magnetic field. The observed dHvA frequency is proportional to this 'extremal area'. In most cases these occur at obvious symmetry points in the reciprocal unit cell, although the origin of some orbits is more subtle. Several papers [7,9,8] have reported calculations of the dHvA extremal cross-sections and effective masses, and generally these are in good agreement with each other.

In Fig. 1, we show the Fermi surface of MgB_2, calculated using the Wien2K package [10] (see later). We have indicated the locations of the predicted dHvA orbits [7,9,8]. These have been labelled $F_1 \ldots F_6$ in accordance with previous publications [11,12,13,14].

3. Experimental details

The Landau level quantization of the energy levels of a metal in a strong magnetic field leads to oscillations of the density of states as a function of the magnetic field and thus to corresponding oscillations in the physical properties [1]. The most popular technique is to measure the oscillations in the differential magnetic susceptibility of the sample. In practice, the sensitivity of this technique is limited by the volume of the sample. In the case of MgB_2, the available highest quality single crystals are relatively small ($<0.05 mm^3$), so better signal to noise can be obtained by measuring the oscillations in the torque, using a piezo-resistive cantilever of the type developed for atomic force microscopy [15]. All the results we will show here were obtained by this method. The details of the method are described in Ref. [12].

4. Results for pure MgB_2

The first report of dHvA oscillations in MgB_2 was by Yelland *et al.* [11]. In this report, which used magnetic fields up to 18 T, three dHvA frequencies (F_1,

F_2, and F_3) were observed. F_1 and F_2 correspond to the extrema of the smaller (light hole) σ tube, and F_3 is located on the electron-like π sheet. In a later study on crystals produced from isotopically pure ^{10}B, Carrington *et al.*[13] observed oscillations from all four sheets of the Fermi surface ($F_1 \ldots F_6$ in Fig. 1), using fields up to 33 T at the Tallahassee high magnetic field laboratory.

The observed dHvA frequencies as a function of field angle are shown in Fig. 2. Results for two different samples are shown. Sample B was grown from natural (mixed isotope) boron whereas sample K was the pure ^{10}B sample. In crystal K signals from all four sheets of the Fermi surface were observed, however, in crystal B no oscillations arising from the larger (heavy hole) σ sheet were observed even in these higher fields. This is almost certainly because of the longer mean-free-paths on the σ sheets of crystal K relative to those in B (see Table 1). Note the opposite trend of ℓ on the π sheets of the two crystals. In general, we find that the mean-free-paths on the σ sheet are not well correlated with those on the π sheets. This will be discussed later.

The dHvA frequencies, extrapolated by polynomial fits to the symmetry points F^0, are given in Table 1. We find very good reproducibility between samples from different sources, and the dHvA frequencies agree to within 30 T or 0.06% of the basal area of the first Brillouin zone ($\frac{\hbar}{2\pi e}\frac{8\pi^2}{\sqrt{3}a^2} = 50.2\,\mathrm{kT}$). This is evidence against there being any significant Mg deficiency in the samples. In general, the agreement between the measured F^0 values and those predicted by theory is very good although not perfect. To investigate the size of the discrepancy we apply a rigid shift to the calculated energies of the σ and π bands. Since the dHvA band mass is defined as $m_B = \frac{\hbar^2}{2\pi}\frac{\partial A}{\partial E}$, the necessary band shifts are given by $\Delta E = \frac{\hbar e}{m_B}\Delta F$ (where $\Delta F = F_{\mathrm{LDA}} - F_{\mathrm{exp}}$). For the σ sheet orbits (1,2,5,6) the average shift is 83 ± 4 meV, whereas for the π sheet orbits (3,4) it is -61 ± 5 meV. The volumes of the c-axis tubes are proportional to the average of the two extremal areas [8] and these are both $\sim 16\%$ smaller than the calculations [16], implying a corresponding difference in the number of holes in these two tubes [8].

In Fig. 3 we compare the frequencies observed experimentally with the predictions based on the LDA band structure. Here we have re-calculated the band structure using the Wien2K package [10] (using parameters similar to those of Kortus *et al.* [3]) on a very dense k-mesh (95000 points in the full Brillouin

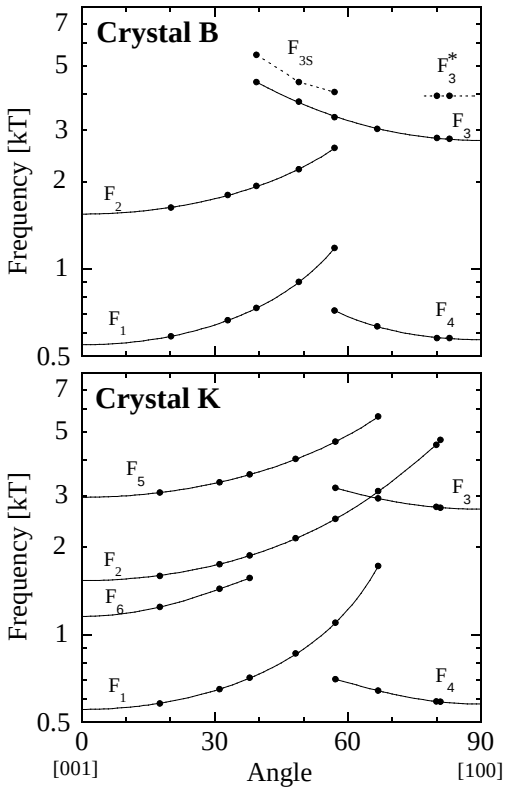

Fig. 2. Observed frequencies versus field angle as the samples were rotated from $H\|c$ to (approximately) $H\|a$. The solid lines are polynomial fits , and the dotted lines are guides to the eye.

zone) and extracted the dHvA parameters using an automated numerical search algorithm. The bands have been rigidly shifted to give the best agreement at the symmetry points as described above. The agreement is excellent, showing that the LDA calculations (with an applied small rigid shift) give the correct Fermi surface.

In MgB_2 the dominant source of mass enhancement is the electron-phonon interaction [5,6,9]. If we assume this is the only source of enhancement we can estimate the electron-phonon coupling constants λ^{ep}, from the measured quasiparticle effective masses m^*, $\lambda^{\mathrm{ep}} = m^*/m_B - 1$. The results (Table 1) show that the values of λ^{ep} on both the σ sheets are approximately a factor three larger than those on the π sheets, in agreement with theoretical predictions. This is a key factor in the multi-band nature of superconductivity in MgB_2, and results in a much larger superconducting gap on the σ sheets than on the π sheets.

The experimental values of λ^{ep} are generally

Table 1
Summary of dHvA parameters for both samples (K and B) along with the theoretical predictions (Th) [9]

Orbit		Crystal K									Crystal B			
		$F^0_{\rm exp}$ [T]	$F_{\rm Th}$ [T]	ΔF [T]	ΔE [meV]	ℓ [Å]	$m^*_{\rm exp}$ [m_e]	$m_{\rm band}$ [m_e]	$\lambda^{\rm ep}_{\rm exp}$	$\lambda^{\rm ep}_{\rm Th}$	$F^0_{\rm exp}$ [T]	ℓ [Å]	$m^*_{\rm exp}$ [m_e]	$\lambda^{\rm ep}_{\rm exp}$
1	σ	551	730	+179	+83	550	0.548 ± 0.02	0.251	1.18 ± 0.1	1.25	546	380	0.553 ± 0.01	1.20 ± 0.04
2	σ	1534	1756	+222	+82	900	0.610 ± 0.01	0.312	0.96 ± 0.03	1.25	1533	580	0.648 ± 0.01	1.08 ± 0.03
3	π	2705	2889	+184	−67	570	0.439 ± 0.01	0.315	0.40 ± 0.03	0.47	2685	680	0.441 ± 0.01	0.40 ± 0.03
4	π	576	458	−118	−56	–	0.31 ± 0.05	0.246	0.31 ± 0.1	0.43	553	–	0.35 ± 0.02	0.42 ± 0.08
5	σ	2971	3393	+422	+79	390	1.18 ± 0.04	0.618	0.91 ± 0.07	1.16	–	–	–	–
6	σ	1180	1589	+409	+87	–	1.2 ± 0.1	0.543	1.2 ± 0.2	1.16	–	–	–	–

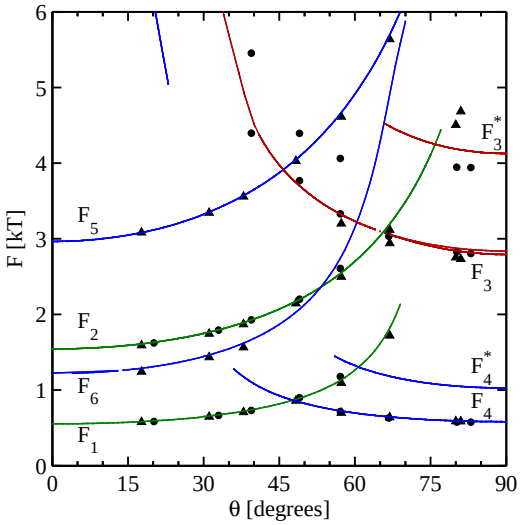

Fig. 3. (color) Comparison of the observed dHvA frequencies with extremal FS areas extracted from the calculated band structure (▲=crystal K, ●=crystal B). Calculated frequencies are for an in-plane angle $\phi = 12°$, to match crystal B.

slightly smaller than the theoretical ones (even when the σ and π band shifts, mentioned above, are taken into account [13]. One possible reason for this is that these theoretical values do not take into account phonon anharmonicity, which has been shown to reduce the average value of λ by around 20% [17].

In sample B, two additional dHvA frequencies were observed which we did not see in crystal K (these are labelled F_3^* and F_{3s}). When the field is aligned in-plane, close to the a-axis [100], the orbit F_3 can be seen, but in addition there are also two orbits in the symmetrically equivalent section of Fermi surface running along the [110] and [0$\bar{1}$0] directions, inclined at 60° to the main F_3 orbit. The origin of F_{3s} has not yet been conclusively identified.

As far as we know, there has been only one other report of dHvA measurements in MgB_2 by another group. Isshiki *et al.* also used a piezoresistive cantilever method to measure crystals grown by an encapsulation technique [14]. Their results are very similar to those shown above for crystal B (Fig. 2). They observe all the same frequencies (including F_3^* and F_{3s} in Fig. 2), but do not see any signals from the heavy hole σ sheet (F_5 and F_6), most likely because of a lower mean-free-path in these samples. The frequencies at the symmetry points (F^0_N) are within 20T of those in Table 1 except F_4 which is 46 T lower [18].

5. Results for Al-doped MgB_2

Studies of the effect of atomic substitutions in MgB_2 are important for applications and may provide a route to improve its superconducting properties. It also allows us to test theoretical understanding of the material. The two elements which substitute most readily in MgB_2 are Al and C which replace Mg and B respectively, to give $Mg_{1-x}Al_x(B_{1-y}C_y)_2$. Both dopants add electrons to the material, and cause T_c to decrease in a similar way [19]. However, the effect of each dopant on H_{c2} and resistivity is very different. Al doping gives a moderate increase in the residual resistivity and causes only a small change in H_{c2} and its anisotropy. On the other hand, carbon doping dramatically increases both the resistivity and H_{c2} [20,21]. This is understandable as the σ band has most weight on the boron plane, whereas the π band has weight on both the boron and magnesium planes. It is therefore to be expected that replacing boron with carbon should strongly increase the scattering rates on both the σ and π bands, but replacing Mg with Al would mainly affect the π band.

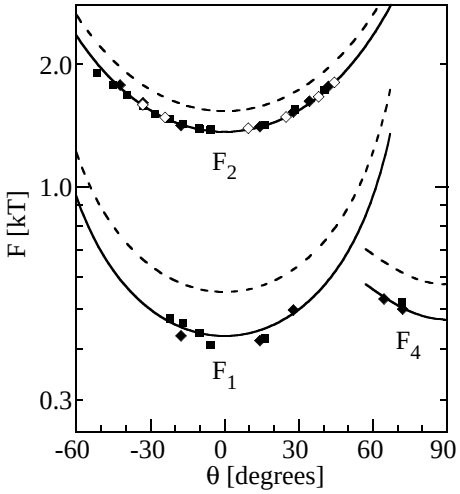

Fig. 4. Observed dHvA frequencies versus angle for the two Al doped samples AN215 (■,♦) and AN217 (◇). Dashed lines are $F(\theta)$ for pure MgB_2, solid lines are pure $F(\theta)$ data scaled to fit the Al doped data.

dHvA studies can test theoretical predictions by measuring sheet-specific scattering rates and by determining quantitatively how doping changes the volumes (or cross-sections) of Fermi surface sheets and the effective masses of quasiparticles. The latter can indicate the doping-dependence of the electron-phonon coupling constants.

Attempts were made to detect dHvA oscillations in both Al and C doped samples with similarly reduced T_c [22]. The C doped samples had T_c values of 35.7 K and 34.5 K, and nominal C contents of $y = 3\%$ and $y = 4\%$ respectively. Their residual resistivities $\rho(T_c)$ were $11\mu\Omega\,$cm and 30 $\mu\Omega\,$cm, substantially larger than for pure MgB_2 which typically has $\rho(T_c) \sim 1\mu\Omega\,$cm. No dHvA signals from either the σ or π sheets were seen in either C doped sample. The two Al doped samples (AN215 and AN217) both had $T_c \simeq 33.6$ K (as determined by heat capacity measurements), and Al contents of $x = 7.9 \pm 0.4\%$ and $x = 7.4 \pm 0.4\%$ (as determined from their c-axis lattice parameters [23]). The residual resistivity of the Al doped samples was found to be $\sim 4.5\ \mu\Omega\,$cm.

In Fig. 4 we show the observed dHvA frequencies versus field angle, θ. Only signals arising from the small (light hole) σ sheet were observed. This sheet has the smallest cross-section (or k_F) so the increased scattering (or decreased ℓ) has the smallest effect on the Dingle damping term. The values of F_1^0 and F_2^0 are the same in both Al doped crystals, and are $10-20\%$ smaller than the corresponding values for pure MgB_2 (see Table 2). Studies on

Table 2
Calculated (LDA)[9] and measured dHvA frequencies [$F^0 \equiv F(\theta = 0)$] for pure [13] and Al doped MgB_2. ΔE is the rigid band shift needed to bring the theoretical values in line with experiment.

		LDA	Pure		AN215		AN217
Orbit		F^0	F^0	ΔE	F^0	ΔE	F^0
		[T]	[T]	[meV]	[T]	[meV]	[T]
F_1	σ	730	546±20	85	410±20	148	···
F_2	σ	1756	1533±20	93	1360±20	147	1360±20
F_3	π	2889	2685±20	-75	···	···	···
F_4	π	458	553±10	-45	480±40	-10	···

many different samples of pure MgB_2 (from different sources) have revealed remarkably reproducible dHvA frequencies and so the measured reduction in cross-section is significant. Within a rigid band shift model our results imply that at this doping the σ bands have shifted to lower energy by ∼70 meV relative to the experimental results for the pure samples. From the calculated volume of these sheets we find that there are $16 \pm 2\%$ fewer holes in 7% Al doped samples compared to pure MgB_2.

This simple analysis was improved considerably by J. Kortus [19,22] who calculated the effect of Al doping on the band structure using the virtual crystal approximation (VCA). Here the effect of doping with Al is simulated by replacing the Mg atom with a virtual atom with charge $Z = xZ_{\rm AL} - (1-x)Z_{\rm Mg}$. These calculations [22] give the following dependence of dHvA frequencies on Al content x, $F_1 = 540 - 1820x$, $F_2 = 1530 - 2050x$ (here the bands have been rigidly shifted to give agreement with the experimental data at $x = 0$, i.e. for pure MgB_2). The observed frequencies (F_1 and F_2) correspond to a doping of $x = 7.5 \pm 1\%$ and $8.4 \pm 1\%$ respectively. These values compare favorably to the x values deduced from the c-axis lattice constant of the same crystal ($\overline{x} = 7.7 \pm 0.4\%$), and so we conclude that the VCA results accurately describe the band filling effect of Al doping in MgB_2.

The VCA calculations are also able to predict the decrease in T_c expected from the doping. For each doping the density of states, phonon frequencies and electron-phonon coupling parameters were calculated. Close to $x = 0$ the calculations [19] predict $dT_c/dx = -0.50$ K/%, and hence for $x = 7.7\%$ we expect a T_c reduction of 4.0 ± 0.3 K. The actual T_c reduction in our samples was 3.9 K, in excellent agreement with the calculations. Note that these calculations do not include the effect of the increased

scattering, so it would appear that, at least for this doping level, the scattering has a minimal effect on T_c.

A further test is to look at the decrease in the measured electron-phonon coupling strength with doping. For the Al doped samples, the only orbit where we have sufficient accuracy to make a meaningful comparison is F_2. For this orbit we find that $\lambda_{\rm ep}$ is $10 \pm 5\%$ smaller than for the pure case (the quoted error includes the measured variation in $\lambda_{\rm ep}$ between different pure samples) [22]. In calculating this we have taken into account the small change in the band mass with doping. Theoretically, it is found that $\lambda_{\rm ep}$ does not vary substantially within each σ sheet and only varies by $\sim 7\%$ between the two σ sheets [9], so the observed reduction in $\lambda_{\rm ep}$ measured on orbit F_2 is expected to be representative of the changes on the other σ sheet. For $x = 7.7\%$, the VCA calculation [19,22] gives $\lambda^{\sigma}_{\rm ep} = 1.16$, which is $\sim 5\%$ smaller than for $x = 0$. This is consistent with our observations.

The mean-free-path, estimated from the Dingle term R_D, was $\ell = 270$ Å for orbit F_2. This is approximately half of that found for pure samples of MgB_2 (grown with natural mixed-isotope boron). The signal from the electron-like π sheet (frequency F_3) is normally large for fields oriented near the plane, [11,13] and as we have not observed this orbit in either Al doped sample we conclude that the mean-free-path on this sheet must be reduced by a somewhat larger factor ($\gtrsim 3$).

Using this information we can make some simple estimates of the effect of Al doping on H_{c2}. In the clean limit, $\mu_0 H_{c2} = \Phi_0/(2\pi\xi^2)$, where ξ can be estimated from the BCS coherence length $\xi_0 = \hbar v_F/(\pi\Delta)$. At low temperature the σ sheets dominate [24,25,26,27] and the anisotropy of H_{c2} ($\gamma_{H_{c2}}$) is determined by the anisotropy of v_F on the σ sheets, i.e., $\gamma_{H_{c2}} = H^{\|a}_{c2}/H^{\|c}_{c2} = \sqrt{\langle v^2_{F,a}\rangle/\langle v^2_{F,c}\rangle}$. In the dirty limit, the same result is found [25] provided the scattering is isotropic. LDA calculations show that for $x \lesssim 0.3$, [26,28]

$$\sqrt{\langle v^2_{F,a}\rangle/\langle v^2_{F,c}\rangle} \simeq 5.9 - 7.5x. \qquad (1)$$

Experimentally, we find for pure MgB_2, $\mu_0 H^{\|c}_{c2} = 3.5\pm0.2$T and $\gamma_{H_{c2}} = 5.5\pm0.2$, at $T \simeq 0.3$K, whereas for our Al doped samples ($x = 7\%$), $\mu_0 H^{\|c}_{c2} = 3.5 \pm 0.1$T and $\gamma_{H_{c2}} = 4.6 \pm 0.2$. These values are in line with other studies [29,26,27,30,21,31]. Eq. (1) slightly overestimates the anisotropy; however, the agreement improves if we take into account the fact that pure MgB_2 has smaller σ tubes compared to the LDA calculations. The hole doping of the σ sheets for pure MgB_2 is roughly equivalent to that in the LDA calculations with $x \simeq 11\%$, so the predicted $\gamma_{H_{c2}}$ has a value of 5.2 for the pure case and 4.6 for the Al doped (x=7%) case. These latter values are in good agreement with experiment. In addition, using the values of Δ and v_F for the σ sheets, $\xi_0 \simeq 130$Å. This is less than ℓ on these sheets for both the pure and x=7% samples and hence the lack of significant change in $\mu_0 H_{c2}(T = 0)$ is also understandable. In other words the σ bands for both the 0% and 7% Al-doped samples are moderately clean ($\xi_0 \lesssim \ell$).

6. Angle dependence of dHvA amplitude

The angular dependence of the dHvA amplitude is often used to extract information about the strength of electron-electron interactions. The Lifshitz-Kosevich expression describing dHvA oscillations in a paramagnetic metal contains a factor $R_S = \cos[\frac{1}{2}\pi g(1+S)m_{\rm B}/m_e]$ which arises from the phase difference between dHvA oscillations from the spin-split Fermi surfaces [1]. Here, S is the Stoner enhancement due to the electron-electron interactions that enhance the Pauli spin susceptibility. At certain field angles, oscillations from the spin-split Fermi surface sheets may destructively interfere; R_S then vanishes and a 'spin-zero' is observed in the dHvA amplitude. Measurement of the field-angle $\theta_{\rm sz}$ for a spin-zero can then be used to determine the Stoner enhancement $S = (2/g)(n+\frac{1}{2})m_e/m_{\rm B}(\theta_{\rm sz}) - 1$, as long as the band-mass $m_{\rm B}(\theta)$, n and g are known. n can often be deduced from the frequency of the 'spin-zeros' as a function of angle; $m_{\rm B}(\theta)$ is taken from LDA band structure calculations.

Fig. 5 shows the dHvA amplitude versus field angle for orbits F_1, F_2 and F_3. The dips in the amplitudes of F_1 and F_2 are due to spin-zeros [13]; fits to the LK expression including $R_{\rm S}$ (solid line) are in excellent agreement with the data. The Stoner enhancements are estimated to be $S(\rm F_1) = 0.10$ and $S(\rm F_2) = 0.14$ [32]. These are approximately a factor 2 lower than the values from band structure calculations [9]. The dHvA values are more consistent with conduction electron spin resonance measurements of the spin susceptibility [33], which imply no enhancement ($S = 0$) to within the experimental error of $\pm15\%$.

A sharp minimum in the amplitude of the F_3 orbit

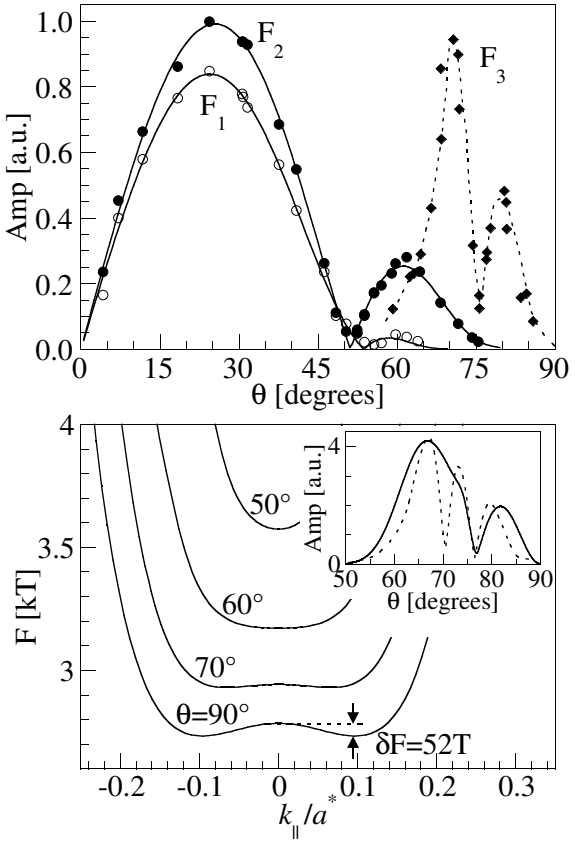

Fig. 5. Top panel: dHvA torque amplitude versus angle for frequencies F_1, F_2 and F_3 ($17.8 < B < 18.0$ T). For frequencies F_1 and F_2 the solid lines are fits to the LK expression including the spin-splitting factor R_S. For F_3 the dotted line is a guide to the eye. Bottom panel: $F(k_\parallel) = \hbar A(k_\parallel)/2\pi e$ for certain field angles, from LDA calculations. For fields close to the boron plane, both minimal and maximal cross–sections are present, but for $\theta < 65°$ there is only one extremal orbit. Inset: the amplitude of F_3 fitted using a two frequency model (solid line) and calculated from the LDA band-structure (dashed line, see text).

on the π band sheet was also observed (at $\theta \approx 74°$, $\phi = 0°$). This was initially interpreted as a spin-zero [11,12,13], although this required an anomalously large Stoner enhancement. A later detailed dHvA study [34] revealed that the dip is in fact due to a small warping of the nearly cylindrical part of this sheet which can be seen in LDA calculations (see Fig. 5). This warping means that there are two extremal dHvA orbits which have very similar frequencies for $\theta > 74°$. For lower θ only a single frequency is observed. Fits of the observed angular dependence using a model with two discrete frequencies separated by $\Delta F \simeq 1.4(\theta - 70°)$ T can reproduce a sharp minimum (see Fig. 5), but are not completely satisfactory [34]. It is well known that the extremal orbit approximation used in the LK formula breaks down when there are significant regions of the Fermi surface over which $F(k_\parallel)$ varies by $\lesssim B$, so that changes in the dHvA phase cannot be treated as $\gg 2\pi$. The effect is predominant in metals with a quasi-two-dimensional Fermi surface [35,36], but it is also significant in the nearly cylindrical sections of the electron-like π band Fermi surface sheet in MgB_2.

Fig. 5 shows $F(k_\parallel) = \hbar A(k_\parallel)/2\pi e$ [where $A(k_\parallel)$ is the Fermi surface cross-sectional area], calculated from LDA results, at several field angles. For angles $\geq 65°$, $F(k_\parallel)$ has two distinct extremal values. The contribution of this finite Fermi surface region to the dHvA amplitude can be calculated by evaluating the integral $I(B) = \int dk_\parallel \sin\left[\frac{2\pi F(k_\parallel)}{B}\right]$ over a suitable range of $k_\parallel$. The inset of Fig. 5 shows the dHvA torque amplitude calculated in this way, taking account of the angle dependence of R_D, R_S and $\mathrm{d}F/\mathrm{d}\theta$. The calculated amplitude has a series of sharp minima which resemble the single minimum seen in the experimental data. The reason for the discrepancy in the number and angular location of the minima is most likely due to a small inaccuracy of the LDA calculation: a warping approximately 30 T smaller than that predicted by the LDA (at $\theta = 90°$) would place the first minimum at the experimentally observed angle (other minima would be shifted to angles where strong damping would prevent their observation). This level of error in the LDA calculation is entirely plausible because the value predicted for F_3 is ~ 200 T too high before applying a rigid energy shift. The absence of a true spin-zero for $\theta \gtrsim 50°$ implies a Stoner enhancement $S < 0.22$, in agreement with other estimates.

7. Damping in the superconducting state

In strongly type II, high H_{c2}, superconductors, quantum oscillations can often be observed in the superconducting state, i.e., at fields where superconducting vortices penetrate the sample (see for example, Ref. [37]). In pure MgB_2, $\mu_0 H_{c2} \sim 18$ T for fields oriented close to the boron planes, and for field angles $\theta \gtrsim 65°$ we are able to observe dHvA oscillations from the π band orbit F_3 below H_{c2} [38]. Fig. 6 shows an example of torque data obtained close to H_{c2}. Quantum oscillations are superimposed on the background torque due to superconductivity, which arises from the anisotropy of the coherence length and pinning [39]. As is generally found in other mate-

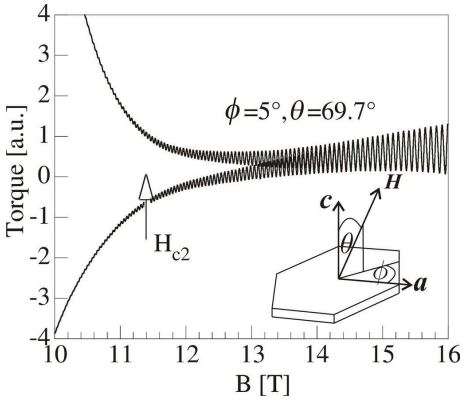

Fig. 6. Torque measured near T_c with $\theta = 69.7°$ and $\phi \simeq 5°$. At this angle $H_{c2} \approx 11.5$ T, as estimated from the rest of the torque loop. The substantial irreversibility above this field is probably due to surface superconductivity. Note that this is part of a minor hysteresis loop; in large samples the torque arising from superconductivity is too large to measure over a complete loop.

rials, the dHvA frequency remains identical to that in the normal state but the oscillations suffer an additional attenuation beyond the factors accounted for in the conventional Lifshitz-Kosevich treatment.

The survival of quantum oscillations deep into the superconducting state is surprising for several reasons: (i) the vortex state is characterized by an intrinsic field inhomogeneity on the scale of the London penetration depth, (ii) pinning of vortices leads to a vortex density gradient and thus field inhomogeneity on the scale of the sample, and (iii) the opening of the superconducting gap modifies the low energy quasiparticle spectrum, reducing the number of carriers available to undergo cyclotron motion. Despite this, oscillations can sometimes be seen at fields as low as 0.2 H_{c2} [40]. A great deal of theoretical work [41] (see Ref. [42] for a review) has been performed to establish whether the origin of the oscillations is the same as that in the normal state, and to understand the mechanisms which attenuate the oscillations. Many models attribute the attenuation to the reduction in the (spatially averaged) density of states at the Fermi energy in the vortex state[43], which is related to the orbit-averaged superconducting gap. This is particularly interesting as the size and $\boldsymbol{k}$-dependence of the additional damping might be used to determine the $\boldsymbol{k}$-dependence of the superconducting gap. Rigorous experimental tests of the various theoretical models for damping of quantum oscillations in the superconducting state have been hard to perform because such observations are generally made in exotic materials where even the normal state is not well understood: in some cases only a fraction of Fermi surface is detected (even in the normal state) and the nature of the effective mass renormalization is unknown. Our knowledge of the electronic structure and superconducting properties of MgB_2, make this an ideal material for performing such a study.

A common way of isolating the additional attenuation is by dividing out other field dependent factors from the original LK expression (see Ref. [38] for details). This additional damping factor, $R_{\rm sc}$, is shown in Fig. 7 for MgB_2. The results were found to be similar at all measured angles, apart from changing the field values at which the attenuation begins. The attenuation has a rather rounded onset, but is quite severe, corresponding to an order of magnitude, at 0.9 H_{c2}.

The value at which attenuation becomes significant is substantially lower than the point at which the torque becomes irreversible. In fact, as shown in Fig. 7, irreversibility extends to much larger fields than is expected from the rest of the superconducting torque loop. This is most likely due to surface superconductivity [14,44], although some calculations suggest that fluctuation effects may be important in this region [45].

The field dependence of R_{sc} was found to be independent of sweep direction, i.e., unaffected by the irreversibility of the background torque, and was reproduced in other samples with different degrees of vortex pinning. This suggests that the signal is unaffected by inhomogeneity of the the vortex distribution due to pinning. Following the arguments in Ref. [37], it is clear that the small scale field inhomogeneity due to a homogenous vortex lattice also does not produce significant attenuation of the dHvA signal in MgB_2.

In another study of this effect in MgB_2 [14], an ac field was superimposed on the main field and modulations in torque were detected. If vortices are pinned at the sample surfaces, the ac field modulation does not penetrate the bulk of the sample and an additional damping of the observed signal results. The dc field torque method used in the work described here [38] is not affected by this problem.

The damping of the dHvA signal is closely linked with the onset of superconductivity in the bulk of the sample. In the present case, additional attenuation seen in the dHvA signal is attributed to the finite gap present on the π band, which is present even in fields close to H_{c2}. Very few probes of the superconducting gap exist in such high fields, and

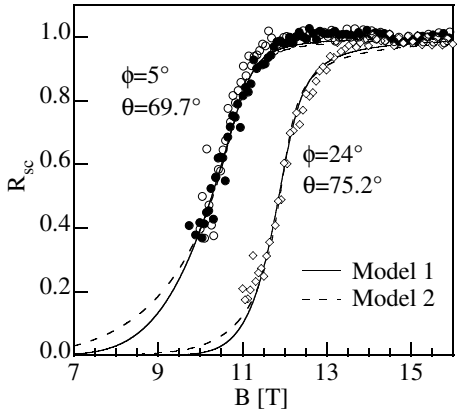

Fig. 7. Additional attenuation of the oscillatory torque signal in MgB_2 in the superconducting (sc) state. For $\theta = 69.7°$, data taken on up sweeps (○) and down sweeps (●) are shown. Data are shown for in-plane rotations $\phi = 5°$ and $\phi = 24°$. Due to fine details of the π-band Fermi surface sheet (see text), measurements at $\phi = 24°$ allow $R_{\rm sc}$ to be determined over a wider field range.

in fact it was previously suggested that the superconductivity in the π bands was quenched at much lower fields [46].

In Fig. 7 two models are applied to the measured damping. The zero field superconducting gap Δ_0 and H_{c2} are free parameters. An additional parameter is included to account for the broadening of the transition [47]. The first model [48] is based on the calculation of the average density of states in the vortex lattice [43]. This requires Δ_0 ∼200-300 K in order to describe the data. An alternative model [49], simply based on the zero field (and hence fully gapped) density of states, requires a value of $\Delta_0 \sim$ 30-60 K, closer to that expected in MgB_2. Compared to results in other materials[37] this level of agreement is not unusual. While this may indicate that this effect has yet to be fully understood, we also note that there are some limitations in this analysis. Firstly, data are only available at high fields, requiring a substantial extrapolation of the field dependence of the gap back to the zero field value. This field dependence is non-trivial in the multi-band case [50]. In addition, the meaning of the gap parameter in each model can be different, i.e., it represents an effective gap, which may be quantitatively different from the zero field value. In the light of this, it would be interesting to observe dHvA signals below H_{c2} on both σ and π bands in MgB_2 to confirm that the relevant parameter is the sheet-dependent (orbit-averaged) gap. This would require the dHvA signal to survive down to fields of order $\mu_0 H_{c2}^{\|c} \simeq$ 3.5T. We estimate that this would require samples with σ sheet mean-free-paths approximately three times larger than we measured to date [38].

8. Conclusions

In conclusion, we have seen that in general, our measurements are in excellent agreement with the predictions of the LDA band structure, including the strength of the electron-phonon coupling on each Fermi surface sheet. The minor discrepancies which remain can be explained with small rigid band shifts. Our work on Al substitution confirms that adding Al dopes electrons into the structure, and reduces the size of the σ sheets. The size of the reduction and the size of the T_c decrease is *quantitatively* explained by the VCA calculations.

Although our understanding of the dHvA data obtained until now is rather good, the data for Al doped samples show that there is scope for further studies of crystals lightly doped with other elements. These would give important insight as to how the mean-free-paths on various orbits and the strengths of the electron-phonon coupling can be altered in a controlled manner with alloying and give deeper understanding as to how T_c and H_{c2} can be optimized for applications.

The dHvA effect in the superconducting state, however, is still not fully understood. The existence of two distinct gaps in MgB_2 gives us an important new parameter with which to study this effect - especially if in the future higher purity samples become available so that dHvA oscillations can be measured at fields less than $\mu_0 H_{c2}^{\|c} \simeq 3.5$T and the superconducting gap on the σ sheet can also be probed.

9. Acknowledgements

High quality single crystal samples were provided by J. Karpinski, S.M. Kazakov and N.D. Zhigadlo of ETH Zürich (pure, Al and C doped MgB_2), and S. Lee, A. Yamamoto, and S. Tajima of University of Tokyo (pure MgB_2). X-ray characterization of the Al-doped samples was performed by J.P.H. Charmant. Important contributions to the dHvA experiments were also made by P.J. Meeson, N.E. Hussey, and L. Balicas. Theoretical work linking the LDA calculations to the dHvA experiments was done by J. Kortus , I.I. Mazin , and H. Harima. Work in the UK was supported by the EPSRC, in Japan by NEDO and in Florida by the NSF.

References

[1] D. Shoenberg, Magnetic Oscillations in Metals, Cambridge University Press, Cambridge, 1984.

[2] I. I. Mazin, V. P. Antropov, Physica C 385 (2003) 49.

[3] J. Kortus, I. I. Mazin, K. D. Belashchenko, V. P. Antropov, L. L. Boyer, Phys. Rev. Lett. 86 (2001) 4656.

[4] J. M. An, W. E. Pickett, Phys. Rev. Lett. 86 (2001) 4366–4369.

[5] H. J. Choi, D. Roundy, H. Sun, M. L. Cohen, S. G. Louie, Nature 418 (2002) 758.

[6] A. Y. Liu, I. I. Mazin, J. Kortus, Phys. Rev. Lett. 87 (2001) 087005.

[7] H. Harima, Physica C 378 (2002) 18.

[8] H. Rosner, J. M. An, W. E. Pickett, S. L. Drechsler, Phys. Rev. B 66 (2002) 024521.

[9] I. I. Mazin, J. Kortus, Phys. Rev. B 65 (2002) 180510.

[10] P. Blaha, K. Schwarz, G. K. H. Madsen, D. Kvasnicka, J. Luitz, WIEN2k, An Augmented Plane Wave + Local Orbitals Program for Calculating Crystal Properties, Karlheinz Schwarz, Techn. Universität Wien, Austria, 2001, ISBN 3-9501031-1-2.

[11] E. A. Yelland, J. R. Cooper, A. Carrington, N. E. Hussey, P. J. Meeson, S. Lee, A. Yamamoto, S. Tajima, Phys. Rev. Lett. 88 (2002) 217002.

[12] J. R. Cooper, A. Carrington, P. J. Meeson, E. A. Yelland, N. E. Hussey, L. Balicas, S. Tajima, S. Lee, S. M. Kazakov, J. Karpinski, Physica C 385 (2003) 75.

[13] A. Carrington, P. J. Meeson, J. R. Cooper, L. Balicas, N. E. Hussey, E. A. Yelland, S. Lee, A. Yamamoto, S. Tajima, S. M. Kazakov, J. Karpinski, Phys. Rev. Lett. 91 (2003) 037003.

[14] T. Isshiki, H. Maruyama, N. Kimura, T. Nojima, A. Ochiai, H. Aoki, Physica C 417 (2005) 110.

[15] C. Rossel, P. Bauer, D. Zech, J. Hofer, M. Willemin, H. Keller, J. Appl. Phys. 79 (1996) 8166.

[16] I. I. Mazin, O. K. Andersen, O. Jepsen, O. V. Dolgov, J. Kortus, A. A. Golubov, A. B. Kuz'menko, D. Van der marel, Phys. Rev. Lett. 89 (2002) 107002.

[17] H. J. Choi, D. Roundy, H. Sun, M. L. Cohen, S. G. Louie, Phys. Rev. B 66 (2002) 020513.

[18] H. Aoki, Personal communication.

[19] J. Kortus, O. V. Dolgov, R. K. Kremer, A. A. Golubov, Phys. Rev. Lett. 94 (2005) 027002.

[20] S. M. Kazakov, R. Puzniak, K. Rogacki, A. V. Mironov, N. D. Zhigadlo, J. Jun, C. Soltmann, B. Batlogg, J. Karpinski, Phys. Rev. B 71 (2005) 024533.

[21] J. Karpinski, N. D. Zhigadlo, G. Schuck, S. M. Kazakov, B. Batlogg, K. Rogacki, R. Puzniak, J. Jun, E. Muller, P. Wagli, R. Gonnelli, D. Daghero, G. A. Ummarino, V. A. Stepanov, Phys. Rev. B 71 (2005) 174506.

[22] A. Carrington, J. D. Fletcher, J. R. Cooper, O. J. Taylor, L. Balicas, N. D. Zhigadlo, S. M. Kazakov, J. Karpinski, J. P. H. Charmant, J. Kortus, Phys. Rev. B 72 (2005) 060507.

[23] J. Karpinski, S. M. Kazakov, J. Jun, N. D. Zhigadlo, M. Angst, R. Puzniak, A. Wisniewski, Physica C 408-10 (2004) 81.

[24] P. Miranovic, K. Machida, V. G. Kogan, J. Phys. Soc. Jpn. 72 (2003) 221.

[25] A. A. Golubov, A. E. Koshelev, Phys. Rev. B 68 (2003) 104503.

[26] M. Putti, C. Ferdeghini, M. Monni, I. Pallecchi, C. Tarantini, P. Manfrinetti, A. Palenzona, D. Daghero, R. S. Gonnelli, V. A. Stepanov, Phys. Rev. B 71 (2005) 144505.

[27] M. Angst, S. L. Bud'ko, R. H. T. Wilke, P. C. Canfield, Phys. Rev. B 71 (2005) 144512.

[28] G. Profeta, A. Continenza, S. Massidda, Phys. Rev. B 68 (2003) 144508.

[29] A. Rydh, U. Welp, A. E. Koshelev, W. K. Kwok, G. W. Crabtree, R. Brusetti, L. Lyard, T. Klein, C. Marcenat, B. Kang, K. H. Kim, K. H. P. Kim, H. S. Lee, S. I. Lee, Phys. Rev. B 70 (2004) 219905.

[30] J. D. Fletcher, A. Carrington, O. J. Taylor, S. M. Kazakov, J. Karpinski, Phys. Rev. Lett. 95 (2005) 097005.

[31] T. Klein, L. Lyard, J. Marcus, C. Marcenat, P. Szabo, Z. Hol'anovo, P. Samuely, B. W. Kang, H. J. Kim, H. S. Lee, H. K. Lee, S. I. Lee, Phys. Rev. B 73 (2006) 224528.

[32] These factors are slightly higher than the ones reported in Ref. [34] ($S(\mathrm{F}_1) = 0.07$ and $S(\mathrm{F}_2) = 0.12$). The difference arises because in Ref. [34] we used the raw bandstructure values of $m_B(\theta)$ whereas here we have used the values calculated from the bands which have been rigidly shifted to agree with the $F(\theta)$ data. This shows the sensitivity of determination of S to uncertainties in the bandstruture - particularly for high angles.

[33] F. Simon, A. Janossy, T. Feher, F. Muranyi, S. Garaj, L. Forro, C. Petrovic, S. L. Bud'ko, G. Lapertot, V. G. Kogan, P. C. Canfield, Phys. Rev. Lett. 87 (2001) 047002.

[34] A. Carrington, J. D. Fletcher, H. Harima, Phys. Rev. B 71 (2005) 174505.

[35] Y. Yoshida, A. Mukai, R. Settai, K. Miyake, Y. Inada, Y. Onuki, K. Betsuyaku, H. Harima, T. D. Matsuda, Y. Aoki, H. Sato, J. Phys. Soc. Jpn. 68 (1999) 3041.

[36] C. Bergemann, S. R. Julian, A. P. Mackenzie, S. Nishizaki, Y. Maeno, Phys. Rev. Lett. 84 (2000) 2662.

[37] T. J. B. M. Janssen, C. Haworth, S. M. Hayden, P. Meeson, M. Springford, A. Wasserman, Phys. Rev. B 57 (1998) 11698.

[38] J. D. Fletcher, A. Carrington, S. M. Kazakov, J. Karpinski, Phys. Rev. B 70 (2004) 144501.

[39] V. G. Kogan, Phys. Rev. B 38 (1988) 7049.

[40] M. Heinecke, K. Winzer, Z. Phys. B-Condens. Mat. 98 (1995) 147.

[41] K. Yasui, T. Kita, Phys. Rev. B 66 (2002) 184516.

[42] T. Maniv, Rev. Mod. Phys. 73 (2001) 867.

[43] U. Brandt, W. Pesch, L. Tewordt, Z. Phys 201 (1967) 209.

[44] A. Rydh, U. Welp, J. M. Hiller, A. E. Koshelev, W. K. Kwok, G. W. Crabtree, K. H. P. Kim, K. H. Kim, C. U. Jung, H. S. Lee, B. Kang, S. I. Lee, Phys. Rev. B 68 (2003) 172502.

[45] T. Maniv, V. Zhuravlev, J. Wosnitza, O. Ignatchik, B. Bergk, P. Canfield, Phys. Rev. B 73 (2006) 134521.

[46] D. Daghero, R. S. Gonnelli, G. A. Ummarino, V. A. Stepanov, J. Jun, S. M. Kazakov, J. Karpinski, Physica C 385 (2003) 255.

[47] N. J. Clayton, H. Ito, S. M. Hayden, P. J. Meeson, M. Springford, G. Saito, Phys. Rev. B 65 (2002) 064515.

[48] K. Maki, Phys. Rev. B 44 (1991) 2861.
[49] K. Miyake, Physica B 188 (1993) 115.
[50] S. Graser, T. Dahm, N. Schopohl, Phys. Rev. B 69 (2004) 014511.